Bose-Einstein condensation in trapped bosons: A variational Monte Carlo analysis

J. L. DuBois and H. R. Glyde
Department of Physics and Astronomy, University of Delaware, Newark, Delaware 19716
(Received 14 March 2000; revised manuscript received 22 August 2000; published 5 January 2001)

Several properties of trapped hard-sphere bosons are evaluated using variational Monte Carlo techniques. A trial wave function composed of a renormalized single-particle Gaussian and a hard-sphere Jastrow function for pair correlations is used to study the sensitivity of condensate and noncondensate properties to the hard-sphere radius and the number of particles. Special attention is given to diagonalizing the one-body density matrix and obtaining the corresponding single-particle natural orbitals and their occupation numbers for the system. The condensate wave function and condensate fraction are then obtained from the single-particle orbital with the highest occupation. The effect of interaction on other quantities such as the ground-state energy, the mean radial displacement, and the momentum distribution is calculated as well. Results are compared with mean-field theory in the dilute limit.

DOI: 10.1103/PhysRevA.63.023602 PACS number(s): 03.75.Fi

I. INTRODUCTION

The spectacular demonstration of Bose-Einstein condensation (BEC) in gases of alkali-metal atoms ^{87}Rb, ^{23}Na, ^{7}Li confined in magnetic traps [1–3] has led to an explosion of interest in confined Bose systems. Of interest is the fraction of condensed atoms, the nature of the condensate, the excitations above the condensate, the atomic density in the trap as a function of temperature, and the critical temperature of BEC, T_c. The extensive progress made up to early 1999 is reviewed by Dalfovo *et al.* [4].

A key feature of the trapped alkali-metal and atomic hydrogen systems is that they are dilute. The characteristic dimensions of a typical trap for ^{87}Rb is $a_{ho}=(\hbar/m\omega_{\perp})^{1/2}=(1-2)\times10^4$ Å (Ref. [1]). The interaction between ^{87}Rb atoms can be well represented by its *s*-wave scattering length, a_{Rb}. This scattering length lies in the range $85<a_{\mathrm{Rb}}<140a_0$, where $a_0=0.5292$ Å is the Bohr radius [5]. The definite value $a_{\mathrm{Rb}}=100a_0$ is usually selected and for calculations the definite ratio of atom size to trap size $a_{\mathrm{Rb}}/a_{ho}=4.33\times10^{-3}$ is usually chosen [4]. A typical ^{87}Rb atom density in the trap is $n\simeq10^{12}-10^{14}$ atoms/cm^3 giving an interatom spacing $l\simeq10^4$ Å. Thus the effective atom size is small compared to both the trap size and the interatom spacing, the condition for diluteness (i.e., $na_{\mathrm{Rb}}^3\simeq10^{-6}$, where $n=N/V$ is the number density). In this limit, although the interaction is important, dilute gas approximations such as the Bogoliubov theory [6], valid for small na^3 and large condensate fraction $n_0=N_0/N$, describe the system well. Also, since most of the atoms are in the condensate (except near T_c), the Gross-Pitaevskii equation [7,8] for the condensate describes the whole gas well. Effects of atoms excited above the condensate have been incorporated within the Popov approximation [9]. One of the chief purposes of this paper is to go beyond the dilute limit, to test the limits of these approximations and to explore the properties of the trapped Bose gas as na^3 increases between the dilute limit and the dense limit. We use variational Monte Carlo (VMC) methods. We increase the density by increasing both N and the *s*-wave scattering length up to the value $na^3\simeq0.21$, which describes liquid ^{4}He at saturated vapor pressure (SVP) when the ^{4}He atoms are represented by hard spheres of diameter $a=2.203$ Å [10].

In addition to the mean-field theories noted above, the trapped Bose gas at finite temperatures has been investigated using path integral Monte Carlo (PIMC) methods. Krauth [11] simulated 10 000 atoms in a spherical trap with the ratio of scattering length a to trap length given by $a/a_{ho}=4.3\times10^{-3}$ noted above. He showed that the critical temperature T_c is lowered compared to the ideal Bose gas as a result of interaction. T_c is lower because the repulsion between the atoms spreads the atoms in the trap and lowers the density compared to the noninteracting case. The same result has been obtained in mean-field approximations [4]. Krauth also showed that, in the dilute limit, the condensed atoms are highly concentrated at the center of the trap while the uncondensed or thermal atoms are spread out over a wide range, are dilute, and are well approximated by a classical, ideal gas. There is little interaction between the condensed and uncondensed components (see also [4]).

Grüter *et al.* [12] evaluated T_c for a uniform, bulk, hard-sphere Bose gas over a wide density range, from dilute to liquid ^{4}He densities. They find that T_c is increased above the ideal Bose gas value by interaction in the dilute range. In the uniform gas case, the density is not changed by interactions. At liquid ^{4}He densities, T_c is decreased by interaction [13,14].

Holzmann *et al.* [15] made a direct comparison between Hartree-Fock (HF) and PIMC calculations of the number density $N(r)$ of atoms in a trap. The atoms were again represented by hard spheres with $a/a_{ho}=0.0043$. From $N(r)$, they find for temperatures near T_c that the condensate fraction N_0 is larger in the exact PIMC evaluation than in the HF approximation. The energy beyond the Hartree-Fock approximation is often denoted as the ''correlation'' energy. This correlation apparently allows N_0 to increase at a given T and allows condensation to begin at a higher temperature. At lower temperature $T\lesssim0.75T_c$, there is excellent agreement between the PIMC and HF $N(r)$. The increase in N_0 with an exact representation of the interaction effects is consistent

with the corresponding increase in T_c with interaction in the uniform Bose gas.

Giorgini *et al.* [16] have evaluated the ground-state energy E/N and the condensate fraction N_0/N at $T=0$ K of a uniform Bose gas over a wide density range ($10^{-6} \leqslant na^3 \leqslant 10^{-1}$) using Green-function Monte Carlo (GFMC) methods. They find that the mean-field results of E/N and the Bogoliubov result for N_0/N agree well with the GFMC values in the density range $10^{-6} \leqslant na^3 \leqslant 10^{-3}$. However, there are clear differences at higher densities $na^3 \geqslant 10^{-3}$ (helium density is $na^3 \simeq 0.21$). The results are not sensitive to reasonable variation of the interboson potential [16].

In this context, we have evaluated the ground-state properties of a trapped, hard-sphere Bose gas over a wide range of densities using VMC methods. We begin in the dilute limit, small N and $a/a_{ho}=0.0043$ corresponding to ^{87}Rb in a trap, and increase both N and a separately to increase the density up to liquid ^{4}He densities. At the lower densities we compare the energy E/N and root-mean-square amplitudes $\langle x^2+y^2 \rangle$ and $\langle z^2 \rangle$ of atoms in an anisotropic trap with Gross-Pitaevskii (GP) results [17]. The two methods agree well at low densities but even at densities $na^3 \approx 10^{-5}$ small differences in E/N are readily apparent. Also, at higher densities we find that the effects of interaction depend separately on N and a/a_{ho}, not simply in the product Na/a_{ho} as it appears in the GP theory. As density is increased still further, we find that the condensate is no longer concentrated at the center of the trap. Rather increased interaction (increased a/a_{ho}) depletes the condensate at the center and the condensate appears at the edges of the trap, as found in liquid ^{4}He droplets (Lewart *et al.* [18]). Also, as density increases, correlations in the single-particle density appear, reflecting the interaction in a confined space, in the same way that interaction at higher density introduces correlation in the pair correlation function in the uniform case. We evaluate the momentum distribution and condensate fraction over the dilute to dense range and compare with mean-field results [19].

In Sec. II, we introduce the Hamiltonian, the wave function, and the MC method and the definition of the natural orbitals. The results are presented in Sec. III and discussed in Sec. IV.

II. BOSONS IN A HARMONIC TRAP

A. The system

We consider N bosons of mass m confined in an external trapping potential, $V_{\rm ext}(\mathbf{r})$, and interacting via a two-body potential $V_{\rm int}(\mathbf{r}_1,\mathbf{r}_2)$. The Hamiltonian for this system is

$$H=\sum_i^N \left(\frac{-\hbar^2}{2m}\boldsymbol{\nabla}_i^2 + V_{\rm ext}(\mathbf{r}_i) \right) + \sum_{i<j}^N V_{\rm int}(\mathbf{r}_i,\mathbf{r}_j). \qquad (1)$$

We consider both a spherically symmetric (S) harmonic trap and an elliptical (E) harmonic trap,

$$V_{\rm ext}(\mathbf{r}) = \begin{cases} \frac{1}{2}m\omega_{ho}^2 r^2 & (S) \\ \frac{1}{2}m[\,\omega_{ho}^2(x^2+y^2)+\omega_z^2 z^2] & (E). \end{cases} \qquad (2)$$

Here ω_{ho}^2 defines the trap potential strength. In the case of the elliptical trap, $V_{\rm ext}(x,y,z)$, $\omega_{ho}=\omega_\perp$ is the trap frequency in the perpendicular or xy plane and ω_z the frequency in the z direction. The mean-square vibrational amplitude of a single boson at $T=0$ K in the trap (2) is $\langle x^2 \rangle = (\hbar/2m\omega_{ho})$ so that $a_{ho} \equiv (\hbar/m\omega_{ho})^{1/2}$ defines the characteristic length of the trap. The ratio of the frequencies is denoted $\lambda=\omega_z/\omega_\perp$ leading to a ratio of the trap lengths $(a_\perp/a_z)=(\omega_z/\omega_\perp)^{1/2}=\sqrt{\lambda}$.

We represent the interboson interaction by a pairwise, hard-core potential,

$$V_{\rm int}(r) = \begin{cases} \infty, & r \leqslant a \\ 0, & r > a, \end{cases} \qquad (3)$$

where a is the hard-core diameter of the bosons. Clearly, $V_{\rm int}(r)$ is zero if the bosons are separated by a distance r greater than a but infinite if they attempt to come within a distance $r \leqslant a$.

The weak interaction limit is $a \ll a_{ho}$ and $a \ll n^{-1/3}$ (where $n=N/V$ is the local number density), a hard-core diameter small compared to the dimensions of the trap and compared to the interparticle spacing $l=(V/N)^{1/3}$. For trapped alkali-metal atoms, we have typically $na^3 \lesssim 10^{-5}$. Introducing lengths in units of a_{ho}, $r \to r/a_{ho}$, and $\hbar\omega_{ho}$ as units of energy as in [4], the Hamiltonian is

$$H=\sum_i^N \frac{1}{2}(-\boldsymbol{\nabla}_i^2 + x_i^2 + y_i^2 + \lambda^2 z_i^2) + \sum_{i<j} V_{\rm int}(|\mathbf{r}_i-\mathbf{r}_j|). \qquad (4)$$

Since there is Bose condensation, we have $n\lambda_T^3 \gtrsim 2.616$, where λ_T is the atomic thermal wavelength. Thus we are in the regime where the atomic wavelength is long compared to the hard-core diameter, $\lambda_T \gg a$ or $ka \ll 1$, where $k \equiv 2\pi/\lambda_T$. The scattering of two particles interacting via a hard-core potential in the limit $ka \ll 1$ is purely s wave with scattering length a. If we approximate the full potential between the two particles by a contact potential,

$$v(r)=g\,\delta(\mathbf{r})=\frac{4\pi\hbar^2 a}{m}\,\delta(\mathbf{r}), \qquad (5)$$

the scattering length in this limit between the two is again purely s wave with scattering length a. Thus we may compare directly results calculated using a hard-core potential (3) and with a contact potential approximation (5) in the regime $a \ll \lambda_T$. Specifically, we may compare the present MC results with results calculated using Eq. (5) and the mean field, Gross-Pitaevskii (GP) equation. This comparison is especially interesting in the dilute limit $na^3 \ll 1$. At high densities ($na^3 \gtrsim 0.1$), we expect short-range, pair correlations induced by the hard core to be important and short-range correlations are not well described by a mean-field theory.

B. Wave function

To describe the ground state of the N bosons, we introduce a variational trial wave function which is a product of a single-particle function $g(\mathbf{r})$ and a pair Jastrow function [20] $f(|\mathbf{r}_1-\mathbf{r}_2|)$,

$$\Psi_\nu(\mathbf{r}_1\cdots\mathbf{r}_N,\alpha,\beta)=\prod_i g(\alpha,\beta,\mathbf{r}_i)\prod_{i<j} f(a,|\mathbf{r}_i-\mathbf{r}_j|), \quad (6)$$

where α and β are the variational parameters. We select a single-particle function,

$$g(\alpha,\beta,\mathbf{r}_i)=\exp[-\alpha(x_i^2+y_i^2+\beta z_i^2)] \quad (7)$$

which is a harmonic oscillator (HO) ground-state function having two variational parameters, α and β. For spherical traps, $\beta=1$, and for noninteracting bosons ($a=0$), $\alpha=1/2a_{ho}^2$. For the pair function we select the exact solution of the Schrödinger equation for two particles interacting via the hard-core potential (3) in the limit $k\to 0$, i.e.,

$$f(a,r)=\begin{cases}\left(1-\dfrac{a}{r}\right), & r>a\\ 0, & r\leqslant a\end{cases} \quad (8)$$

(see, for example, Huang [21]). The $\Psi_\nu(\mathbf{r}_1\cdots\mathbf{r}_N)$ therefore has the correct form for small $|\mathbf{r}_i-\mathbf{r}_j|$ and has two variational parameters α and β that describe the spread of the bosons in the trap as the hard-core diameter is increased. By constructing the wave function in this way, we limit the number of variational parameters while preserving the correct functional form in the $a\to 0$ limit. However, the lack of any variational parameters in the Jastrow term is a potential source of inaccuracy.

We then minimize the expectation value of the Hamiltonian as obtained from

$$\langle H\rangle=\frac{\int d\mathbf{r}_1\cdots d\mathbf{r}_N\Psi_\nu^*\Psi_\nu\left(\dfrac{H\Psi_\nu}{\Psi_\nu}\right)}{\int d\mathbf{r}_1\cdots d\mathbf{r}_N\Psi_\nu^*\Psi_\nu}$$

with respect to α and β using the Metropolis Monte Carlo method of integration. This is accomplished by using a Metropolis random walk [22] to generate a set of N particle configurations, $\Omega_1\cdots\Omega_M$, which conform to the probability distribution $|\Psi_\nu|^2$. We then approximate $\langle H\rangle$ by summing over the ''local energy'' as follows:

$$\langle H\rangle\leqslant\frac{1}{M}\sum_{n=1}^{M}\left(\frac{H(\Omega_n)\Psi_\nu(\Omega_n)}{\Psi_\nu(\Omega_n)}\right).$$

For a review of the variational Monte Carlo method, see [23].

C. Condensate and natural orbitals

A goal here is to calculate the condensate fraction and condensate density in the ground state. To do this, we require a definition of the condensate single-particle state. Following Penrose and Onsager, Löwdin, and others [24,25], we take the one-body density matrix (OBDM) as the fundamental quantity for an interacting system and define the natural single-particle orbitals (NO) in terms of the OBDM.

The OBDM is [26]

$$\rho(\mathbf{r}',\mathbf{r})=\langle\hat{\Psi}^\dagger(\mathbf{r}'),\hat{\Psi}(\mathbf{r})\rangle, \quad (9)$$

where $\hat{\Psi}(\mathbf{r})$ is the field operator that annihilates a single particle at the point $\mathbf{r}$ in the system. At $T=0$ K, the expectation value is evaluated using the wave function $\Psi_\nu(\mathbf{r})$ in Eq. (6). To define the NO, we introduce a set of single-particle states having wave functions $\phi_i(\mathbf{r})$ and expand $\hat{\Psi}(\mathbf{r})$ in terms of the operators $\hat{a}_i$ which annihilate a particle from state $|i\rangle$,

$$\hat{\Psi}_0=\sum_i \phi_i(\mathbf{r})\hat{a}_i. \quad (10)$$

Requiring that the $\hat{a}_i$ satisfy the usual commutation ($[\hat{a}_i^\dagger,\hat{a}_j]=\delta_{ij}$) and number relations ($\langle\hat{a}_i^\dagger\hat{a}_j\rangle=N_i\delta_{ij}$), we have

$$\rho(\mathbf{r},\mathbf{r}')=\Sigma_{ij}\phi_j^*(\mathbf{r}')\phi_i(\mathbf{r})N_i\delta_{ij}=\Sigma_{ij}\phi_j^*(\mathbf{r})\phi_i(\mathbf{r}')N_i\delta_{ij}. \quad (11)$$

This may be taken as the defining relation of the NO, $\phi_i(\mathbf{r})$. Specifically, we have from Eq. (11),

$$\int d\mathbf{r}\cdots d\mathbf{r}'\,\phi_i^*(\mathbf{r})\rho(\mathbf{r},\mathbf{r}')\phi_j(\mathbf{r}')=N_i\delta_{ij}, \quad (12)$$

so that the NO may be obtained by diagonalizing the OBDM. The eigenvectors are the NO and the eigenvalues are the occupation, N_i, of the orbitals. The condensate is the orbital having the highest occupation, denoted $\phi_0(r)$, and the condensate fraction is $n_0=N_0/N$.

The relations (11) and (12) involve the vector $\mathbf{r}$ and $\mathbf{r}'$ and cannot be solved directly as matrix equations. To obtain matrix equations, we restrict ourselves to spherical traps and seek equations for the radial component of the NO. Assuming the potential seen by a single particle, including interparticle interaction, is spherically symmetric, the NO will have the form

$$\phi_i(\mathbf{r})=\phi_{nl}(r)Y_{lm}(\theta,\phi), \quad (13)$$

where $Y_{lm}(\Omega)$ are the spherical harmonics, $\phi_{nl}(r)$ is the radial wave function, and $i=n,l,m$ are the state indices. We expand the OBDM in its angular momentum (l) components $\rho_l(r,r')$ as

$$\rho(\mathbf{r},\mathbf{r}')=\sum_l\frac{(2l+1)}{4\pi}P_l(\hat{\mathbf{r}}\cdot\hat{\mathbf{r}}')\rho_l(r,r'), \quad (14)$$

where $P_l(\cos\theta)$ are Legendre polynomials in the angle between $\hat{\mathbf{r}}$ and $\hat{\mathbf{r}}'$ and

$$\rho_l(r_1,r_1')=\int d\Omega_1 d\mathbf{r}_2\cdots d\mathbf{r}_N \Psi^*(\mathbf{r}_1\cdots\mathbf{r}_N) \times P_l(\hat{r}_1\cdot\hat{r}_1')\Psi(\mathbf{r}_1'\cdots\mathbf{r}_N). \quad (15)$$

Substituting Eqs. (13) and (14) into Eq. (11) and using the properties of the spherical harmonics, $Y_{lm}(\Omega)$, we obtain a relation equivalent to Eq. (11) for each l component $\phi_{nl}(r)$ of the NO,

$$\rho_l(r,r')=\sum_n \phi_{nl}(r)\phi_{nl}(r')N_{nl}, \quad (16)$$

where $i=nl$. To solve this equation readily as a matrix equation, we introduce the radial function

$$u_{nl}(r)=r\phi_{nl}(r). \quad (17)$$

The $u_{nl}(r)$ is well behaved at $r\rightarrow 0$ and has dimensions $L^{-1/2}$ like a one-dimensional wave function. In terms of the $u_{nl}(r)$, the defining relations are

$$[r\rho_l(r_1,r_1')r']=\sum_n u_{nl}(r)u_{nl}^*(r')N_{nl} \quad (18)$$

and

$$\int dr[r\rho_l(r_1,r_1')r']u_{nl}(r')=u_{nl}(r)N_{nl}. \quad (19)$$

The $[r\rho_l(r_1,r_1')r']$ serves as a one-dimensional OBDM along the radial coordinate. This 1D matrix relation may be solved numerically on a grid in r to obtain the $u_{nl}(r)$ as eigenvectors and the N_{nl} as eigenvalues. The condensate orbital is

$$\phi_0(r)=\frac{1}{\sqrt{4\pi}}u_{00}(r)/r. \quad (20)$$

The momentum distribution may be obtained from the OBDM as well given that the orbitals in momentum space are

$$\tilde{\phi}_i(\mathbf{k})=\frac{1}{(2\pi)^{3/2}}\int d\mathbf{r}\, e^{-i\mathbf{k}\cdot\mathbf{r}}\phi_i(\mathbf{r}) \quad (21)$$

and the momentum distribution is

$$\tilde{\rho}(\mathbf{k})=\sum_i n_i|\tilde{\phi}_i(\mathbf{k})|^2. \quad (22)$$

Substituting Eqs. (21) into (22), obtains an expression for $\tilde{\rho}(\mathbf{k})$ in terms of the OBDM:

$$\tilde{\rho}(\mathbf{k})=\frac{1}{(2\pi)^3}\int d\mathbf{r}\, d\mathbf{r}'\rho(\mathbf{r},\mathbf{r}')e^{i\mathbf{k}\cdot(\mathbf{r}-\mathbf{r}')}. \quad (23)$$

The momentum distribution for a spherically symmetric system is therefore

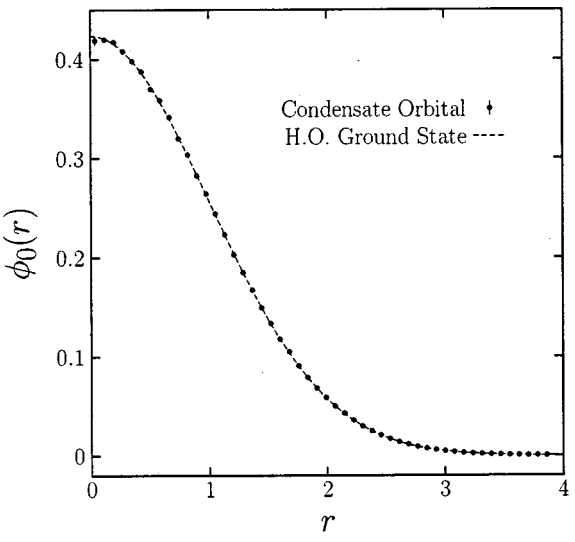

FIG. 1. The condensate orbital, $\phi_0(r)$, obtained by numerical diagonalization of the OBDM $\rho_0(r,r')=\Sigma_i n_i\phi_i^*(r)\phi_i(r')$ calculated by variational Monte Carlo (VMC) (solid dots) for an ideal Bose gas in a harmonic trap. The dashed line is the harmonic-oscillator (HO) ground-state wave function for the same trap. $\phi_0(r)$ and r are dimensionless in units of a_{ho}.

$$\tilde{\rho}(\mathbf{k})=\tilde{\rho}(|\mathbf{k}|) =\frac{1}{2\pi^2}\int d\mathbf{r}_1\cdots d\mathbf{r}_N|\Psi_\nu(\mathbf{r}_1\cdots\mathbf{r}_N)|^2 \times\int_0^\infty dr\, r^2\frac{\sin(kr)}{kr}\frac{\Psi_\nu(\mathbf{r}_1+\mathbf{r},\mathbf{r}_2\cdots\mathbf{r}_N)}{\Psi_\nu(\mathbf{r}_1\cdots\mathbf{r}_N)}, \quad (24)$$

where the orientation of $\mathbf{r}$ may be chosen arbitrarily.

III. RESULTS

In this section we present the results of the present variational Monte Carlo (VMC) calculation of properties of bosons at $T=0$ K confined in a harmonic trap. To begin, Fig. 1 shows the condensate orbital $\phi_0(r)$ for independent, noninteracting bosons in a spherical harmonic trap compared to the harmonic oscillator (HO) ground-state function for the same trap. The $\phi_0(r)$ is calculated by evaluating the one-body density matrix (OBDM) and diagonalizing it numerically to obtain the single-particle orbitals and their occupation as discussed in Sec. II. For no interaction, only $\phi_0(r)$ is occupied ($n_0=1$). The excellent agreement between $\phi_0(r)$ and the HO ground-state function for all r provides a good check of the method for noninteracting bosons. The statistical sample is proportional to r^2 and the statistics become poor at $r\rightarrow 0$.

Figure 2 shows the energy per particle, E/N, of a gas of N weakly interacting hard-sphere bosons in an ellipsoidal trap. The ratio of the characteristic length of the short axis (z axis) to the longer perpendicular (x and y) axis of the trap is $(a_z/z_\perp)=1/\sqrt{\lambda}$; $\lambda=\sqrt{8}$. The hard-sphere diameter a (scattering length) of the bosons corresponds to ^{87}Rb atoms in an ellipsoidal trap with $a/a_{ho}=0.004\,33$ with $a_\perp=a_{ho}$. In Fig.

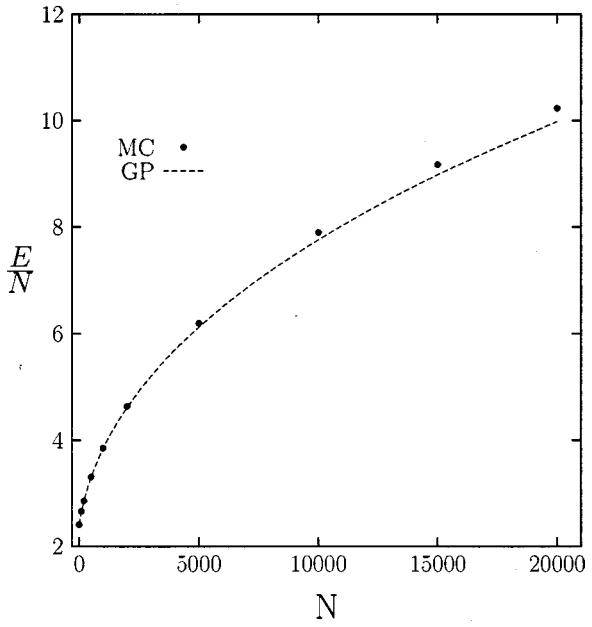

FIG. 2. Energy per particle, in units of $\hbar\omega_\perp$, for hard-sphere bosons in an anisotropic trap as a function of the number of particles N in the trap. Solid circles are the present VMC values for hard spheres with diameter corresponding to the scattering length of Rb, $a_{\mathrm{Rb}}=4.33\times10^{-3}a_{ho}$, where a_{ho} is the trap length in the perpendicular direction. The error bars lie within the solid dots. The dashed line is the value obtained using the Gross-Pitaevskii equation (GP) for the same system [17].

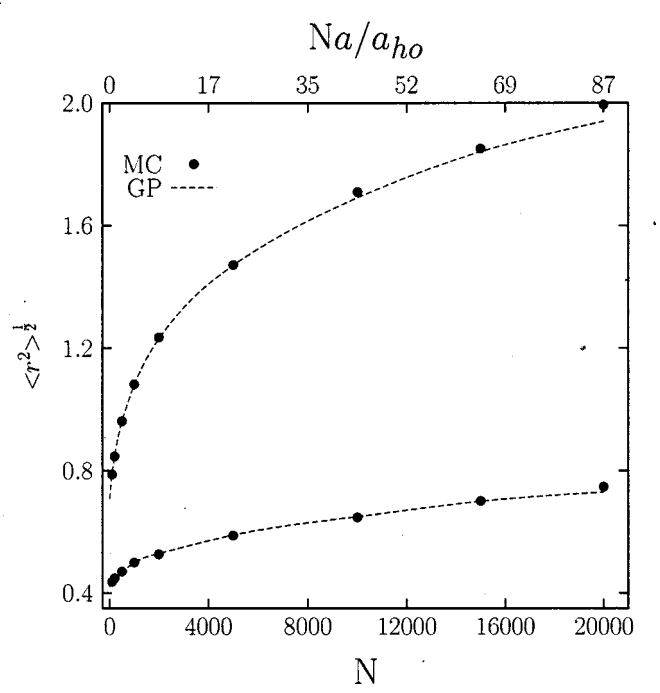

FIG. 3. Average axial displacement of bosons from the center of an anisotropic trap in the $\perp$ direction, $\langle x^2+y^2\rangle^{1/2}$ (top) and in the z direction $\langle z^2\rangle^{1/2}$ (bottom) expressed in units of the perpendicular trap length a_{ho} as a function of the number of particles, N. Solid dots are from the present VMC results for hard spheres with diameter $a_{\mathrm{Rb}}=4.33\times10^{-3}a_{ho}$. The dashed lines are the values obtained from the Gross-Pitaevskii equation (GP) for the same a_{Rb} [17].

2, the dots are the present VMC E/N of the whole Bose gas while the dashed line is the E/N of the condensate calculated by Dalfovo and Stringari [17] using the Gross-Pitaevskii (GP) equation. Our purpose is to make comparisons between the present VMC calculation and GP equation results across the dilute regime for which GP is expected to be valid. The region $100\leqslant N\leqslant 20\,000$ corresponds to atom densities at the center of the trap of $2\times10^{-6}\lesssim na^3\lesssim 2\times10^{-5}$. In the earliest experiments [1] with ^{87}Rb, there were typically $N=10\,000$ atoms in the trap. In more recent experiments N is larger, $N\simeq10^5-10^6$.

At small N values in the dilute limit, there is excellent agreement between the GP and VMC energies. In this regime, the mean-field GP equation is expected to be accurate. As N increases, a clear difference between the VMC and GP E/N values emerges. We find that for a fixed scattering length, the difference $\delta(E/N)=(E_{\mathrm{MC}}-E_{\mathrm{GP}})/N$ is proportional to $N^{3/5}$ and can be well represented as

$$\delta(E/N)=[(3.0\times10^{-5}\pm10^{-6})(N)^{3/5}-0.052]\hbar\omega_\perp . \tag{25}$$

The difference is 1.8% at $N=10\,000$ and 2.5% at $N=20\,000$. The difference, we believe, arises largely because there is excitation of bosons above the condensate. E_{MC}/N includes the excited atoms while E_{GP}/N is the energy of the condensate alone. We return to this point in Sec. IV.

Figure 3 compares the root-mean-square displacement of hard-sphere bosons from the center of the same anisotropic trap discussed in Fig. 2 calculated using VMC and the GP equation. The upper (lower) line is the radial displacement along the $\perp$ (z) direction. The agreement between the GP and the VMC displacements is excellent, right up to $N=20\,000$ for $a=a_{\mathrm{Rb}}$.

It is interesting that the VMC and GP displacements agree well while the energies in Fig. 2 differ for $N\gtrsim10^4$. Essentially, the E/N is very sensitive to the few high-energy bosons at the edges of the trap. That is, the small number of atoms having large displacements increase the energy significantly but change $\langle r^2\rangle$ little. An example of this effect is found in the Thomas-Fermi approximation where the density is cut off to zero at a specific radius [4]. In the TF model, there is no tail in the density reaching up to large r values. The cutoff changes $\langle r^2\rangle$ little but E/N is significantly affected [4].

Figure 4 again shows E/N for hard-sphere bosons in an anisotropic trap as a function of Na/a_{ho}. However, in this case the product Na/a_{ho} is adjusted by varying both N and a/a_{ho}. The star symbols show E/N for $a=a_{\mathrm{Rb}}$ and $2000\leqslant N\leqslant 20\,000$, the crosses are for $a=10a_{\mathrm{Rb}}$ and $200\leqslant N\leqslant2000$, and the square denotes $a=20a_{\mathrm{Rb}}$ and $100\leqslant N\leqslant1000$. If the impact of interaction and E/N depended solely on the product Na/a_{ho}, as is the case in the mean-field GP equation, all three lines in Fig. 4 would coincide. E/N clearly depends separately on N and a/a_{ho}, even in the region of $N=10\,000-20\,000$. The separate dependence is not large at $Na/a_{ho}\approx20$ but becomes increasingly large as Na/a_{ho} increases. Also, at these and larger densities, the parameter

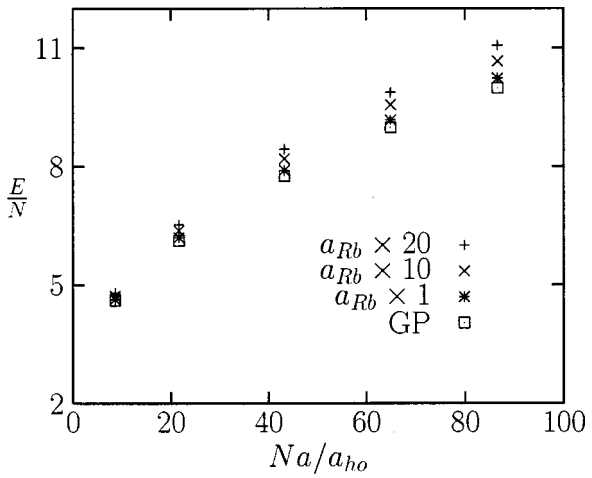

FIG. 4. Energy per particle, in units of $\hbar\omega_\perp$, for interacting bosons in an anisotropic trap as a function of the product Na/a_{ho} (number of particles N and scattering length a) as obtained by the present VMC calculation for hard spheres with core diameter $a=1,10,20$ times the scattering length of ^{87}Rb, $a_{\mathrm{Rb}}=4.33\times10^{-3}a_{ho}$. Open squares are Gross-Pitaevskii equation results for the same Na. Estimated errors lie within symbol size.

which determines the magnitude of corrections arising from interactions is $N^{3/5}(a/a_{ho})^{8/5}$. Apparently, the interaction effects depending on Na/a_{ho} are valid only in the limit of small $a(a/a_{ho}\ll 1)$. We examine the functional form of the separate dependence of E/N on N and a/a_{ho} in Sec. IV.

Having investigated lower densities and made comparisons with results obtained using the GP equation, we now turn to higher densities and bosons represented by hard spheres having larger hard-core diameters. We evaluate the OBDM and the density for these cases going up to densities

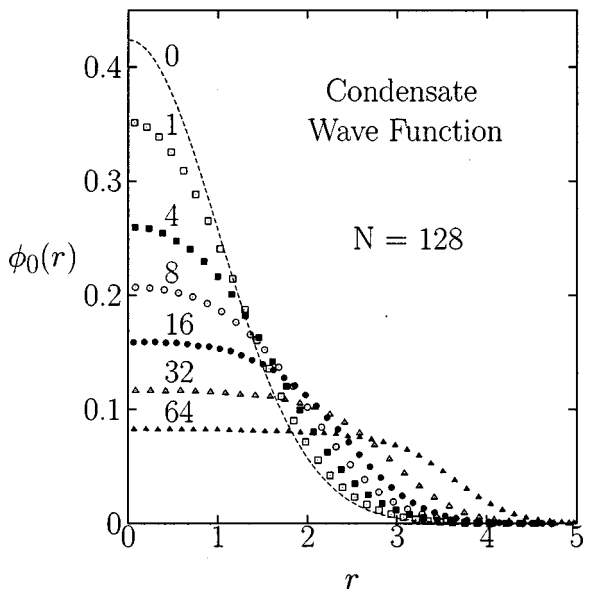

FIG. 5. Condensate natural orbital $\phi_0(r)$ for 128 hard spheres with core diameter $a=0,1,...,64$ times the scattering length of ^{87}Rb, $a_{\mathrm{Rb}}=4.33\times10^{-3}a_{ho}$ in a spherically symmetric harmonic trap. All lengths are in terms of the trap length $a_{ho}=\sqrt{\hbar/m\omega_{ho}}$.

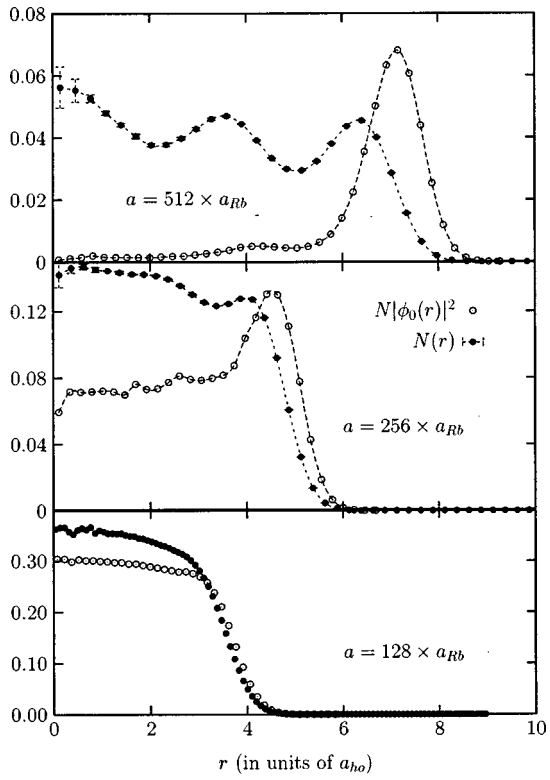

FIG. 6. Condensate density, $|\phi_0(r)|^2$, scaled by the number of particles N, vs total particle density, $N(r)$, with scattering length $a=128,256,512\times a_{\mathrm{Rb}}$, from bottom to top, where $N(r)$ is normalized to N, $|\phi_0(r)|^2$ is normalized to 1, and all lengths are in units of the characteristic trap length a_{ho}.

comparable to liquid ^{4}He droplets. Figure 5 shows the condensate orbital (wave function) for 128 bosons in a spherical harmonic trap as the hard-core radius, a, is increased from zero up to $a=64a_{\mathrm{Rb}}$ ($a_{\mathrm{Rb}}/a_{ho}=0.004\,33$). The case $a/a_{\mathrm{Rb}}=1$ corresponds to $N=128$ Rb atoms in a spherical trap. Clearly, the condensate orbital spreads out in the trap as a increases. At $a/a_{\mathrm{Rb}}=64$, the condensate density is effectively constant in the trap out to nearly three times the trap length parameter a_{ho}. For these larger core radii, the appropriate measure of the interaction is na^3, where $n=N/V$. For $a=64a_{\mathrm{Rb}}$, $na^3\simeq2\times10^{-3}$ at the center of the trap.

In Fig. 6, we show the total density $\rho(r)$ and the density of atoms in the condensate orbital as $N|\phi_0(r)|^2$ for 64 bosons in a spherical trap with a increased to $128a_{\mathrm{Rb}}$, $256a_{\mathrm{Rb}}$, and $512a_{\mathrm{Rb}}$. Since we plot $N|\phi_0(r)|^2$ rather than $N_0|\phi_0(r)|^2$, ''condensate density'' can exceed the total density. At $a=256a_{\mathrm{Rb}}$, the condensate is $n_0=N_0/N=20\%$. We note that as a increases, the condensate moves away from the center of the trap. At $a=512a_{\mathrm{Rb}}$, the condensate is at the edges of the trap. When na^3 is large at the center of the trap, the maximum condensate density is in the region of lower particle density found at the edge of the trap, as calculated for liquid ^{4}He droplets [18]. Thus the location of the condensate is entirely different at small and large scattering length. In a slave boson approach, depletion of the condensate at the center of the trap has also been demonstrated [27]. Also, at large a/a_{ho} the total density develops correlations. These

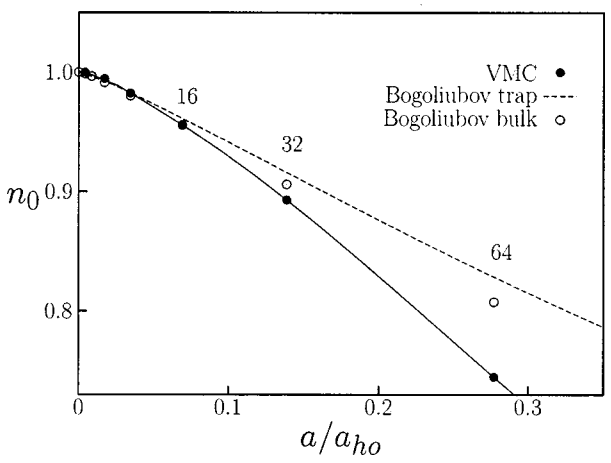

FIG. 7. The condensate fraction, n_0, for 128 particles in a harmonic trap as a function of the ratio of scattering length to trap length a/a_{ho} using three methods. Occupation numbers for the ground-state orbital ϕ_0 found using variational Monte Carlo (MC) methods (solid dots) agree well with values of n_0 obtained from the Bogoliubov equations for a uniform gas (open circles) and a mean-field Bogoliubov approximation (dashed line) [19] for $n_0 > 0.9$.

correlations reflect the interboson correlations induced by the hard-core interaction. For $a = 512 a_{\mathrm{Rb}}$, we have $a/a_{ho} \simeq 2.2$. With a peak in the density at $r = 0$, we expect the first minimum in the density at $r \simeq a/a_{ho} \simeq 2.2$ as in the upper frame of Fig. 6.

Figure 7 gives the fraction of bosons in the condensate orbital, n_0, calculated by VMC and diagonalization of the OBDM corresponding to the condensate orbitals shown in Fig. 5. The n_0 values, as in Fig. 5, are for 128 hard-sphere bosons in a spherical trap with hard-sphere radius $a/a_{\mathrm{Rb}} = 1$, 2, 4, 16, 32, and 64, e.g., $a = 64 \times a_{\mathrm{Rb}} = 64 \times 4.33 \times 10^{-3} a_{ho} = 0.277 a_{ho}$. The Bogoliubov [6] result for n_0 adapted to a spherical trap [19] is shown as a dashed line. Visible departures of the VMC n_0 from the Bogoliubov result begin at $n_0 \simeq 0.96$ (a depletion of 4%) corresponding to a density at the center of the trap $na^3 \simeq 1 \times 10^{-3}$. In the uniform gas case, the Bogoliubov result remains accurate up to a condensate fraction $n_0 \simeq 0.89$ (11% depletion), which occurs at a density $na^3 \simeq 5 \times 10^{-3}$ [16]. The Bogoliubov approximation has a more limited range of application for bosons in a trap because the interaction changes the density profile (and the shape of the condensate wave function) as well as simply depleting the condensate and n_0 depends on the density and shape of the condensate wave function. In the uniform case, the density cannot change. In Fig. 8, we again show the condensate fraction, n_0, as a function of the ratio of the scattering length, a, to the characteristic trap length, a_{ho}. Here, n_0 is given for three different numbers of particles: $N = 64$, 128, and 256. The corresponding value of the particle density, na^3, for the 64-particle case is shown on the top axis for reference. At liquid-helium densities, the condensate fraction is roughly twice that of bulk liquid ^{4}He. This difference can be understood by noting the shape of the radial condensate density shown for the $a = 256 a_{\mathrm{Rb}}$ case in Fig. 6. Here, we see that while the maximum particle density occurs at the center the trap, the condensate density is peaked

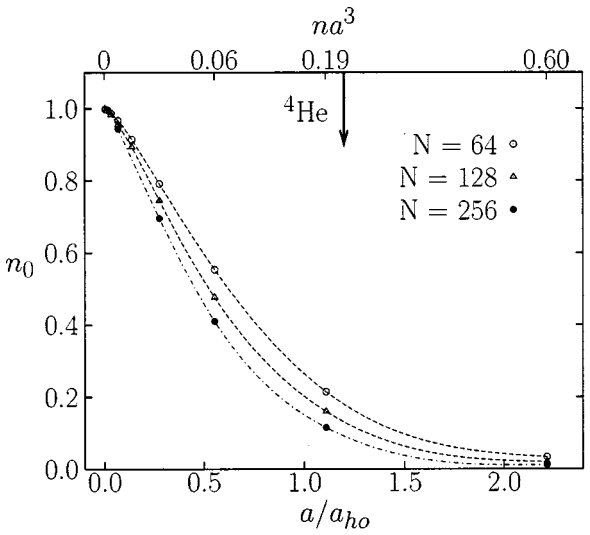

FIG. 8. Condensate fraction, n_0, at zero temperature for interacting hard spheres in a harmonic trap as a function of the hard-sphere diameter, a, in units of the trap length, $a_{ho} = \sqrt{\hbar/m\omega_{ho}}$, for systems with $N = 64$, 128, and 256 particles. The top axis indicates the corresponding values of na^3 found in the center of the trap for the 64-particle system. The arrow indicates the value of a/a_{ho} at which na^3 is the same as liquid ^{4}He at SVP.

in the low-density region at the edge of the cloud. This dilute region allows for a larger fraction of particles to occupy the condensate orbital than in a uniform system at ^{4}He densities.

Figure 9 shows the effect of increased scattering length, a, on the momentum distribution of particles in an isotropic harmonic trap at $T = 0$. The values for the scattering length and the trap configuration under consideration correspond to those shown for the spatial distribution in Fig. 5.

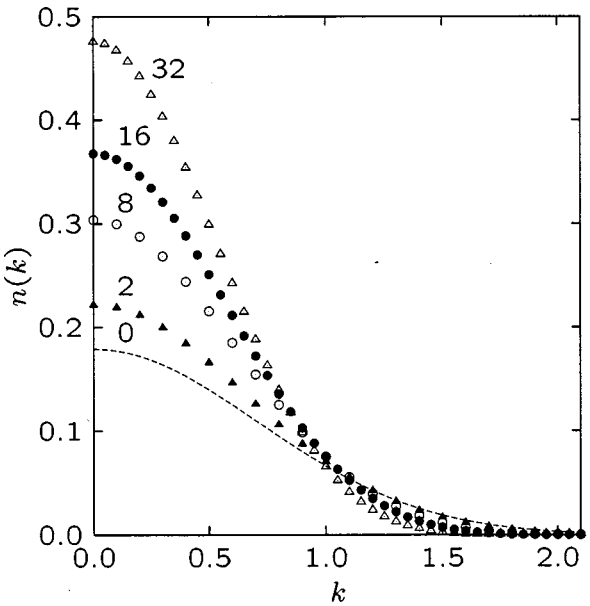

FIG. 9. Momentum distribution, $n(k)$, for 128 hard spheres with diameter $a = 0,1,...,32$ times the scattering length of ^{87}Rb, $a_{\mathrm{Rb}} = 4.33 \times 10^{-3}$, in a harmonic trapping potential. Momentum is in units of the inverse of the characteristic length of the trap $a_{ho}^{-1} = \sqrt{m\omega_{ho}/\hbar}$.

TABLE I. The ratio of the density at the center of the trap calculated using the Thomas-Fermi expression, $n_{\mathrm{TF}}(0)$, and in the present VMC evaluation, $n_{\mathrm{MC}}(0)$, to the density for no interaction, $n_{ho}(0)$. The ratio decreases as the (scattering length)/(hard-core diameter) a/a_{Rb} is increased as shown in Fig. 5.

a/a_{Rb}	Na/a_{ho}	$n_{\mathrm{MC}}(0)a^3$	$n_{\mathrm{TF}}(0)/n_{ho}(0)$	$n_{\mathrm{MC}}(0)/n_{ho}(0)$
1	0.55	1.3×10^{-6}	0.93	0.71
4	2.22	4.3×10^{-5}	0.41	0.38
8	4.43	2.4×10^{-4}	0.27	0.25
16	8.87	1.0×10^{-3}	0.17	0.14
32	17.7	4.3×10^{-3}	0.12	0.075
64	35.5	1.9×10^{-2}	0.077	0.041

IV. DISCUSSION

In this section we compare the present MC values for the density, condensate fraction, and energy of bosons in a trap with mean-field (MF) and Thomas-Fermi (TF) approximation results. The aim is to assess the limits of applicability of the MF and TF expressions and to investigate the origin of any differences between MF and MC values. We start with the density at the center of the trap, $n(0)$, since this density is needed in MF expressions for the depletion of the condensate and for the energy. Also, comparisons [4] of the density calculated in the TF approximation and in mean-field, Gross-Pitaevskii (GP) approximations show that $n_{\mathrm{TF}}(0)$ is accurate for large $Na/a_{ho}(Na/a_{ho}\approx100)$.

The density of N independent bosons in an asymmetric trap is $n_{ho}(\mathbf{r})=\phi_{ho}^2(\mathbf{r})=N/(\pi^{3/2}a_xa_ya_z)\exp[-(x^2/a_x^2+y^2/a_y^2+z^2/a_z^2)]$. For the elliptical trap considered above, $a_x=a_y=a_{ho}$ and $a_z=a_{ho}/\sqrt{\lambda}$, the density at the center of the trap is [4]

$$n_{ho}(0)=Na_{ho}^2a_z/\pi^{3/2}=\sqrt{\lambda}N/\pi^{3/2}a_{ho}^3. \tag{26}$$

The $\phi_0(r)$ for a spherically symmetric trap ($\lambda=1$) is shown in Fig. 1. As interaction is increased (e.g., a/a_{ho} is increased), the $\phi_0(r)$ spreads out and the density $n(0)$ at the center of the trap decreases, as depicted in Fig. 5. For $\lambda=1$, the ratio of the density at the center with interaction to the $n_{ho}(0)$ for no interaction in the TF approximation is

$$\frac{n_{\mathrm{TF}}(0)}{n_{ho}(0)}=\left(\frac{15^{2/5}\sqrt{\pi}}{8}\right)(Na/a_{ho})^{-3/5}. \tag{27}$$

This ratio calculated using MC, $n_{\mathrm{MC}}(0)/n_{ho}(0)$, for increasing scattering length, $a/a_{ho}=Fa_{\mathrm{Rb}}=F\times4.33\times10^{-3}$ with $F=1$, 4, 8, 16, 32, and 64, can be obtained from Fig. 5 and is listed in Table I. The TF ratio agrees well with the MC ratio in the range $4<F<16$ or $2<Na/a_{ho}<10$. We expect the TF result to be inaccurate at small Na/a_{ho} because the TF limit is a large Na/a_{ho} approximation.

In addition, at large Na/a_{ho}, the density exceeds the dilute limit so that all mean-field theories become inaccurate. The dilute limit is exceeded at $n(0)a^3\gtrsim10^{-3}$, which corresponds to $F\geqslant16$ for the gas considered in Table I. Between these limits, however, for $Na/a_{ho}\gtrsim5$ and $n(0)a^3\lesssim10^{-3}$, the $n_{\mathrm{TF}}(0)$ gives a good estimate of the boson number density at the center of the trap.

For a uniform Bose gas, the MF, Bogoliubov theory predicts a condensate fraction $n_0=N_0/N=1-(8/3)\times(na^3/\pi)^{1/2}$, where $n=N/V$ is the uniform density [6]. That is, the fraction of bosons excited out of the condensate is

$$\frac{\delta N}{N}=\frac{N-N_0}{N}=\frac{8}{3}\left(\frac{na^3}{\pi}\right)^{1/2}. \tag{28}$$

The corresponding result for bosons in a spherical harmonic trap is [4]

$$\frac{\delta N}{N}=\frac{5\pi}{8}\left(\frac{n_{\mathrm{TF}}(0)a^3}{\pi}\right)^{1/2}. \tag{29}$$

Figure 7 shows that the mean-field expressions (28) and (29) agree well with the present MC values of n_0 for $N=128$ bosons up to $a/a_{ho}\approx16a_{\mathrm{Rb}}$ or up to $n(0)a^3\approx10^{-3}$. Specifically, for $F=8$ at $n_{\mathrm{MC}}(0)a^3=2.4\times10^{-4}$, the MC value for the depletion in Fig. 7 is $\delta N/N=1.9\%$ while the Bogoliubov result from Eq. (29) is $\delta N/N=1.7\%$. For larger values of $n(0)a^3$, the depletion is significantly underestimated by the Bogoliubov expressions. This agrees with the findings of MC determinations for n_0 in a uniform Bose gas [16]. In the uniform case, Eq. (28) agrees with MC values up to $na^3\approx5\times10^{-3}$ and underestimates depletion at larger na^3. The MF results are accurate up to somewhat higher densities in the bulk probability because the density itself does not depend on the interaction in a uniform Bose gas. Recent experiments [28] have obtained stable condensates at densities corresponding to $na^3\approx10^{-2}$. At this density, the condensate fraction is ≈0.85 and effects resulting from depletion are expected to be significant.

For a uniform Bose gas, the MF Bogoliubov expression for the energy including the leading correction arising from depletion is in units of $\hbar^2/2ma^2$[16]

$$\frac{E}{N}=4\pi na^3\left[1+\frac{128}{15}\left(\frac{na^3}{\pi}\right)^{1/2}\right]. \tag{30}$$

The corresponding TF expression for bosons in a spherical trap ($\lambda=1$) is [4]

$$\frac{E}{N}=\frac{5}{7}\mu_{\mathrm{TF}}\left[1+\frac{7\pi}{8}\left(\frac{n_{\mathrm{TF}}(0)a^3}{\pi}\right)^{1/2}\right], \tag{31}$$

where $\mu_{\mathrm{TF}}=1/2\hbar\omega_\perp(15Na/a_{ho})^{2/5}$ and from Eqs. (26) and (27), $n_{\mathrm{TF}}(0)a^3=(15^{2/5}/8\pi)N^{2/5}(a/a_{ho})^{12/5}$.

The above expressions may be used to estimate the energy of bosons in an anisotropic trap by replacing a_{ho} with the geometric mean $a_g=(a_xa_ya_z)^{1/3}$, which is $a_g=a_{ho}\lambda^{-1/6}$ for the trap discussed in Fig. 2. The energy of independent, noninteracting bosons in this anisotropic trap is

$$(E/N)\rightarrow E_{ho}=\hbar\omega_{ho}(1+\lambda/2)=\hbar\omega_{ho}(2.414) \tag{32}$$

TABLE II. Depletion of the condensate $(\delta N/N)_{\mathrm{MF}}$ calculated using mean-field expansions (29) for the Bose gas considered in Fig. 2 for $N=5000$, 10 000, and 20 000. The $(\delta E/E)_{\mathrm{MC}}$ is the fractional difference between the present MC energy of the gas and the GP [4] energy of the condensate, $\delta E=E_{\mathrm{MC}}-E_{\mathrm{GP}}$. This difference is consistent with the depletion of the condensate and mean-field expressions of $\delta E/E$ arising from depletion.

N	Na/a_{ho}	$n_{\mathrm{TF}}(0)a^3$	$\left(\frac{\delta N}{N}\right)_{\mathrm{MF}}$	$\left(\frac{\delta E}{E}\right)_{\mathrm{MC}}$
5000	21.6	$1.1\times10-5$	0.37%	1.1%
10000	43.3	1.5×10^{-5}	0.43%	1.8%
20000	86.6	2.0×10^{-5}	0.50%	2.5%

$(\omega_{ho}=\omega_{\perp})$. In Fig. 2, (E/N) has the noninteracting boson limit at $N\rightarrow0$. As N increases, (E/N) increases. As seen from Eq. (31), the mean-field energy in the TF approximation $(E/N)_{\mathrm{TF}}=5\mu_{\mathrm{TF}}/7$ increases with N as $(E/N)_{\mathrm{TF}}\propto(Na/a_{ho})^{2/5}$. The $(E/N)_{\mathrm{MC}}$ in Fig. 2 follows the dependence approximately. However, direct evaluation of Eq. (31) shows that $(E/N)_{\mathrm{TF}}$ underestimates the energy significantly, by 25% at $N=20\,000$ $(Na/a_{ho}=86.6)$. Thus while the Thomas-Fermi density $n_{\mathrm{TF}}(0)$ at the center of the trap is accurate, the TF energy is a poor approximation in this density regime. This is because the TF approximation underestimates the density at larger r and the high-energy particles at large r contribute significantly to the energy.

In Fig. 2 we see that the present Monte Carlo E/N lies above the Gross-Pitaevskii E/N, by 2.5% at $N=20\,000$. A difference could arise for two reasons.

First, the MC energy is the E/N of the whole Bose gas while the GP equation calculates the E/N of the condensate only. To investigate the effects of depletion on E/N, we note, comparing Eqs. (28) and (30), that the fractional change in energy arising from depletion, $\delta E/E$, can be related to the fraction of atoms excited out of the condensate as

$$\delta E/E=(128/15)(na^3/\pi)^{1/2}=(16/5)\,\delta N/N \tag{33}$$

in the bulk. The corresponding equation for the trap is, from Eqs. (29) and (31),

$$\delta E/E=(7/5)\,\delta N/N. \tag{34}$$

These are lowest-order expressions. In Table II, we list the depletion of the condensate $\delta N/N$ for the bosons in the anisotropic trap considered in Fig. 2 for $N=5000$, 10 000, and 20 000 predicted by Eq. (29). We expect these predictions to be accurate since $n_{\mathrm{TF}}(0)$ is reliable and $n_{\mathrm{TF}}(0)a^3$ is small. The interaction depletes the condensate 0.5% at $N=20\,000$. From the above connection between δE and δN, the energy (E/N) including depletion is expected to lie 0.7–1.6 % above the energy of the condensate. On this basis, VMC and GP energies are consistent.

To explain the connection between the difference in VMC and GP energies and depletion of the condensate more fully, we have plotted $\delta(E/N)=(E_{\mathrm{MC}}-E_{\mathrm{GP}})/N$ versus Na/a_{ho} in Fig. 10. From Eq. (31), the difference from the mean-field

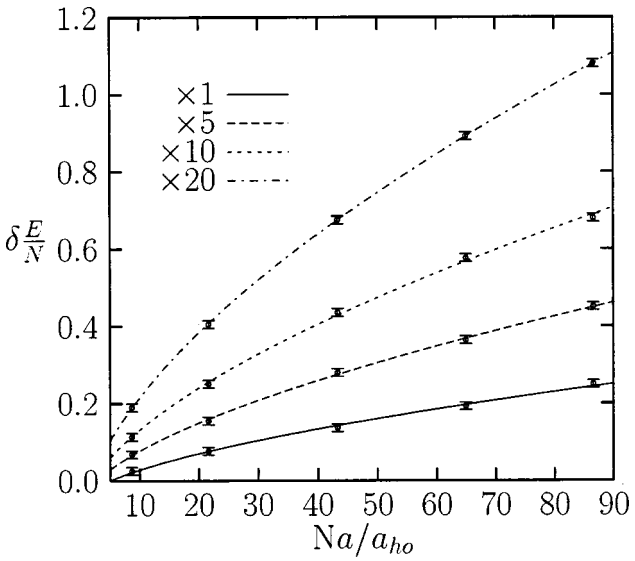

FIG. 10. Energy difference between present VMC and GP results, $\delta E/N$, as a function of Na/a_{ho} for four different values of $a/a_{\mathrm{Rb}}=1$, 5, 10, and 20. The lines are fits of $\delta E/N=m(a/a_{ho})^{8/5}N^{3/5}+b$ to the data points.

energy arising from depletion is

$$\delta(E/N)_{\mathrm{TF}}=(5\pi\mu_{\mathrm{TF}}/8)[n_{\mathrm{TF}}(0)a^3/\pi]^{1/2}\propto^{3/5}(a/a_{ho})^{8/5} \tag{35}$$

in the TF limit. In Fig. 10, we show the difference in the VMC and GP energies, $\delta(E/N)$, versus the product Na/a_{ho}. This difference is obtained from Fig. 4 for four values of $a/a_{ho}=1,5,10,20$. The lines in Fig. 10 are fits of $\delta(E/N)=mN^{3/5}(a/a_{ho})^{8/5}+b$ to the data, where the fitting parameters m and b were allowed to change for each a/a_{ho} value. The good fit of these lines shows that $\delta(E/N)$ reflects the dependence on N expected for a difference in energy arising from exciting bosons out of the condensate. Thus the difference in $(E/N)_{\mathrm{MC}}$ from $(E/N)_{\mathrm{GP}}$ is consistent in magnitude and dependence on N and a/a_{ho} with that expected for an $(E/N)_{\mathrm{MC}}$ that includes bosons both in and above the condensate while $(E/N)_{\mathrm{GP}}$ is the energy of bosons in the condensate only. Thus we believe the MC and GP energies differ chiefly because the MC includes ''excited'' particles while the GP energy does not.

Second, the present VMC E/N is a genuine upper bound for the whole gas and could lie above the whole gas energy. We have not tested the sensitivity of E/N to different choices of the trial wave function. In addition, while the present pair Jastrow function (8) is exact in the dilute limit, it does not contain any variational parameters and is therefore not optimized for trapped hard spheres at higher densities. As a result, at least some of the difference in $(E/N)_{\mathrm{MC}}$ from $(E/N)_{\mathrm{GP}}$ could arise from the present choice of trial wave function. For example, Fabrocini and Polls (FP) have evaluated the whole E/N for bosons in a spherical trap $a_x=a_y=a_z=4.33\times10^{-3}a_{ho}$ using correlated basis function and hypernetted-chain (HNC) methods [29]. Both methods provide estimates of E/N which lie below the present VMC E/N. At $N=10^5$, the density $[n(0)a^3=2.5\times10^{-5}]$ in this

trap is similar to that for $N=2\times10^4$ in the present elliptical trap. At this density, the HNC E/N lies 0.8% above the GP energy of the condensate while the present VMC E/N is 2.5% above GP. FP also consider a mean-field model incorporating quantum depletion which predicts an increase in E/N of 1.2% above the GP result at this density. Generally, the HNC energy in the trap lies below the energy expected for depletion and may be too low. For example, the HNC energy for a uniform gas of bosons lies above the energy expected for depletion. Definite resolution of these differences awaits a model-independent evaluation of E/N by diffusion Monte Carlo methods.

Finally, an important result of the present MC evaluation is that as the boson density na^3 increases, the condensate gradually moves from the center of the trap to the edges of the trap as shown in Fig. 6. At large na^3, the condensate is at the edges of the trap. In this limit, the depletion of the condensate is large and the condensate seeks the regions of lowest total density which are at the surface of the trap. Both the condensed and uncondensed atoms must be included in the calculation to obtain this effect. This result is consistent with the calculations in liquid ^{4}He droplets [18], which find the condensate concentrated at the surface of the droplet.

ACKNOWLEDGMENTS

Stimulating discussions with Charles W. Clark and Timothy Ziman are gratefully acknowledged. J.L.D. acknowledges support from DE-SGGFP NASA Grant No. NGT5-40024.

[1] M. H. Anderson, J. R. Ensher, M. R. Matthews, C. E. Wieman, and E. A. Cornell, Science **269**, 198 (1995).
[2] K. B. Davis, M.-O. Mewes, M. R. Andrews, N. J. van Druten, D. S. Durfee, D. M. Kurn, and W. Ketterle, Phys. Rev. Lett. **75**, 3969 (1995).
[3] C. C. Bradley, C. A. Sackett, J. J. Tolett, and R. G. Hulet, Phys. Rev. Lett. **75**, 1687 (1995); C. C. Bradley, C. A. Sackett, and R. G. Hulet, *ibid.* **78**, 985 (1997).
[4] F. Dalfovo, S. Giorgini, L. Pitaevskii, and S. Stringari, Rev. Mod. Phys. **71**, 463 (1999).
[5] J. R. Gardner *et al.*, Phys. Rev. Lett. **74**, 3764 (1995).
[6] N. N. Bogoliubov, J. Phys. (Moscow) **11**, 23 (1947).
[7] E. P. Gross, Nuovo Cimento **20**, 454 (1961).
[8] L. P. Pitaevskii, Zh. Eksp. Fiz. **40**, 646 (1961) [Sov. Phys. JETP **13**, 451 (1961)].
[9] D. A. W. Hutchinson, E. Zaremba, and A. Griffin, Phys. Rev. Lett. **78**, 1842 (1997).
[10] M. H. Kalos, D. Levesque, and L. Verlet, Phys. Rev. A **9**, 2178 (1974).
[11] W. Krauth, Phys. Rev. Lett. **77**, 3695 (1996).
[12] P. Grüter, D. Ceperley, and F. Laloë, Phys. Rev. Lett. **79**, 3549 (1997).
[13] J. Wilks, *The Properties of Liquid and Solid Helium* (Clarendon Press, Oxford, 1967).
[14] E. L. Pollock and K. J. Runge, Phys. Rev. B **46**, 3535 (1992).
[15] M. Holzmann, W. Krauth, and M. Naraschewski, Phys. Rev. A **59**, 2956 (1999).
[16] S. Giorgini, J. Boronat and J. Casulleras, Phys. Rev. A **60**, 5129 (1999).
[17] F. Dalfovo and S. Stringari, Phys. Rev. A **53**, 2477 (1996).
[18] D. S. Lewart, V. R. Pandharipande, and S. C. Pieper, Phys. Rev. B **37**, 4950 (1988).
[19] J. Javanainen, and S. M. Yoo, Phys. Rev. Lett. **76**, 161 (1996).
[20] R. Jastrow, Phys. Rev. **98**, 1479 (1955).
[21] K. Huang, *Statistical Mechanics* (Wiley & Sons, New York, 1963), p. 276.
[22] N. Metropolis, A. E. Rosenbluth, M. N. Rosenbluth, A. H. Teller, and E. Teller, J. Chem. Phys. **21**, 1087 (1953).
[23] M. P. Nightingale and C. J. Umrigar, *Quantum Monte Carlo Methods in Physics and Chemistry* (Kluwer, Boston, 1999), p. 129.
[24] P. O. Löwdin, Phys. Rev. **97**, 1474 (1955).
[25] L. Onsager and O. Penrose, Phys. Rev. **104**, 576 (1956).
[26] G. Baym, *Lectures on Quantum Mechanics* (W. A. Benjamin, Inc., London, 1976), p. 425.
[27] K. Ziegler and A. Shukla, Phys. Rev. A **56**, 1438 (1997).
[28] S. L. Cornish, N. R. Claussen, J. L. Roberts, E. A. Cornell, and C. E. Wieman, Phys. Rev. Lett. **85**, 1795 (2000).
[29] A. Fabrocini and A. Polls, Phys. Rev. A **60**, 2319 (1999).